

NO-A102 666

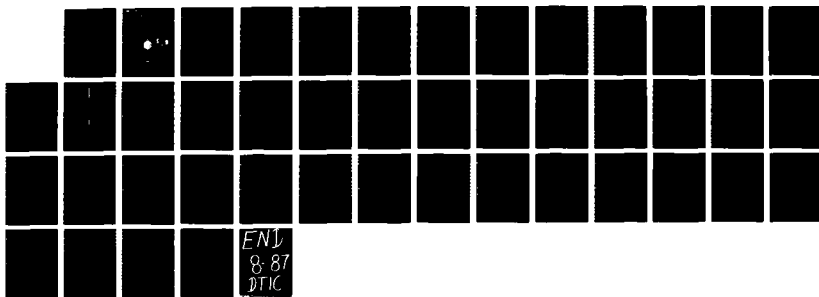
NUCLEAR MAGNETIC RESONANCE IN GALLIUM ARSENIDE(U) NAVAL
ACADEMY ANNAPOLIS MD M F FINCH 19 MAY 87 USNA-TSPR-144

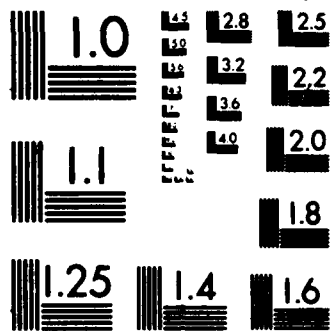
1/1

UNCLASSIFIED

F/G 9/1

NL





MICROCOPY RESOLUTION TEST CHART
NATIONAL BUREAU OF STANDARDS-1963-A

AD-A182 666

A TRIDENT SCHOLAR PROJECT REPORT

NO. 144

"Nuclear Magnetic Resonance in Gallium Arsenide"



DTIC
ELECTE
JUL 24 1987
S D

UNITED STATES NAVAL ACADEMY
ANNAPOLIS, MARYLAND

1987

This document has been approved for public
release and sale; its distribution is unlimited.

87 7 22 003

UNCLASSIFIED

SECURITY CLASSIFICATION OF THIS PAGE (When Data Entered)

A 182 666

REPORT DOCUMENTATION PAGE		READ INSTRUCTIONS BEFORE COMPLETING FORM
1. REPORT NUMBER U.S.N.A. - TSPR; no. 144 (1987)	2. GOVT ACCESSION NO.	3. RECIPIENT'S CATALOG NUMBER
4. TITLE (and Subtitle) NUCLEAR MAGNETIC RESONANCE IN GALLIUM ARSENIDE.		5. TYPE OF REPORT & PERIOD COVERED Final 1986/1987
		6. PERFORMING ORG. REPORT NUMBER
7. AUTHOR(s) Finch, Michael F.		8. CONTRACT OR GRANT NUMBER(s)
9. PERFORMING ORGANIZATION NAME AND ADDRESS United States Naval Academy, Annapolis.		10. PROGRAM ELEMENT, PROJECT, TASK AREA & WORK UNIT NUMBERS
11. CONTROLLING OFFICE NAME AND ADDRESS United States Naval Academy, Annapolis.		12. REPORT DATE 19 May 1987
		13. NUMBER OF PAGES 40
14. MONITORING AGENCY NAME & ADDRESS (if different from Controlling Office)		15. SECURITY CLASS. (of this report)
		15a. DECLASSIFICATION/DOWNGRADING SCHEDULE
16. DISTRIBUTION STATEMENT (of this Report) This document has been approved for public release; its distribution is UNLIMITED.		
17. DISTRIBUTION STATEMENT (of the abstract entered in Block 20, if different from Report) This document has been approved for public release; its distribution is UNLIMITED.		
18. SUPPLEMENTARY NOTES Accepted by the U.S. Trident Scholar Committee.		
19. KEY WORDS (Continue on reverse side if necessary and identify by block number) Gallium Arsenide semiconductors, Semiconductors, Nuclear magnetic resonance spectroscopy, Spectroscopy		
20. ABSTRACT (Continue on reverse side if necessary and identify by block number) Nuclear Magnetic Resonance (NMR) lineshapes of ⁶⁹ Ga in GaAs:In were studied for two different levels of indium dopant. The lineshapes were develop- ed by fourier analysis of the spin echoes. First order quadrupole effects manifested themselves as wings in the lineshapes. As expected the wings were larger in the more heavily doped sample. The dependance of the second moment of the lineshapes on the orientation of the crystal in the field supports a continuous solid model of the strain, in which the strain <u>COVERED</u>		

DD FORM 1 JAN 73 1473

EDITION OF 1 NOV 65 IS OBSOLETE
S N 0102-LF-014-6601

UNCLASSIFIED

SECURITY CLASSIFICATION OF THIS PAGE (When Data Entered)

UNCLASSIFIED

SECURITY CLASSIFICATION OF THIS PAGE (When Data Entered)

attenuates as the cube of the distance from the impurity site. Because of noise levels the model can only be confirmed for distances greater than 10A from the impurity, and no determination of the strain on the first through eighth shells surrounding the impurity can be made.

Keywords:

S N 0102- LF-014-6601

UNCLASSIFIED

SECURITY CLASSIFICATION OF THIS PAGE(When Data Entered)

U.S.N.A. - Trident Scholar project report; no. 144 (1987)

"Nuclear Magnetic Resonance in Gallium Arsenide"

A Trident Scholar Report

by

Midshipman Michael F. Finch, Class of 1987

U.S. Naval Academy

Annapolis, Maryland

Donald J. Treacy

Professor D.J. Treacy - Physics

Accepted for Trident Scholar Committee

Dennis F. Hanson

Chairman

19 May 1987

Date

Accession For	
NTIS CRA&I	<input checked="" type="checkbox"/>
DTIC TAB	<input type="checkbox"/>
Unannounced	<input type="checkbox"/>
Justification	
By	
Distribution/	
Availability Codes	
Dist	Availability for Special
A-1	

USNA-1531-2

ABSTRACT

Nuclear Magnetic Resonance (NMR) lineshapes of ^{69}Ga in GaAs:In were studied for two different levels of indium dopant. The lineshapes were developed by fourier analysis of the spin echoes. First order quadrupole effects manifested themselves as wings in the lineshapes. As expected the wings were larger in the more heavily doped sample. The dependance of the second moment of the lineshapes on the orientation of the crystal in the field supports a continuous solid model of the strain, in which the strain attenuates as the cube of the distance from the impurity site. Because of noise levels the model can only be confirmed for distances greater than 10\AA from the impurity, and no determination of the strain on the first through eighth shells surrounding the impurity can be made.

Table of Contents

	page
ABSTRACT	1
Table of Contents	2
I. Introduction	4
II. Classical NMR Theory	7
A. NMR Signals	7
B. Broadening	8
C. Echoes	13
III. Quantum NMR Theory	16
A. Zeeman Energies	16
B. Dipolar Broadening	19

	page
C. Quadrupolar Broadening	20
D. Pseudodipolar Broadening	26
IV. Experiment	28
V. Results	31
VI. Discussion of Results	36
Notes	40

I. Introduction

Because of their high speeds, III-V semiconductors, are used in many electronic devices. A III-V semiconductor is a crystal with two different elements, one from group III of the periodic table, and one from group V. Examples of III-V semiconductors include gallium arsenide, indium antimonide, and indium phosphide. Dislocation scattering reduces the mobility of the charge carriers and reduces the speed of the semiconductor. The speed of these devices could be improved if the dislocation density could be reduced. By trapping the dislocations, isovalent doping reduces the dislocation density from tens of thousands to a few hundred per square centimeter.¹ Isovalent doping is used, to maintain the properties of the semiconductor; a non-isovalent dopant would function as a donor or an acceptor, creating charged sites within the crystal which would alter the semi-conducting properties of the crystal.

This report describes use of nuclear magnetic resonance (NMR) to determine the effects of isovalent doping in GaAs:In. NMR is highly sensitive in probing the local environment of the resonating nucleus. NMR can show the effects of a wide variety of interactions. In liquids, NMR provides information on molecular bonding. This is a standard diagnostic technique to in chemistry to determine

the number of different bond configurations of the resonant nuclei. In metals, interactions with conduction electrons shift the resonance, this is the Knight shift.¹ This report intends to show how the isovalently doped indium affects GaAs:In crystals as inferred from the changes in the width of the NMR lines as measured by the change in the second moment. ~

NMR is radio-frequency (RF) spectroscopy. In conventional visible-light spectroscopy, the transitions of the atomic electrons appear on the order of few electron volts. In NMR the transitions of the nuclear magnetic moment are of interest; however, because the energies involved are on the order of 10^{-8} electron volts, the emissions are in the radio-frequency region rather than in the visible region of the electromagnetic spectrum. NMR signals can be observed in any material whose atoms have a non-zero magnetic moment. Both isotopes of gallium and the single isotope of arsenic have non-zero moments, so these three species will have NMR spectra. This investigation focussed on the information which could be obtained from the ^{69}Ga resonance.

The theory underlying this study will first be presented classically. Then expanded quantum mechanically, to treat the quadrupolar and dipolar interactions in more detail. After explaining the theory behind this work, the

experimental set up and data taking procedures will be described. The results will then be presented, and finally a discussion of these results will be the last section of this paper.

II. Classical NMR Theory.

A. NMR Signals

A typical NMR sample used in this study consisted of approximately 10^{22} nuclei each of which have a microscopic magnetic moment. These microscopic individual moments can be added together to create a net magnetic moment vector, M . Because this vector is the sum of roughly 10^{22} individual moments, it can be treated classically as a vector having a continuous range of values. With no external field, a microscopic net moment will be randomly oriented, due to incomplete cancellation of the individual moments. Applying an external field creates a net macroscopic moment parallel to the field. For a magnetic field, H_0 , in the z -direction, the magnetic moment in that direction can be written as.²

$$M = \chi H \quad (1)$$

Where χ is the nuclear paramagnetic susceptibility, and is a function of the nuclear spin, the nuclear magnetic moment, the number of nuclei, and the temperature. A coil which has its cylindrical axis in the x -direction then

applies a pulse of short duration. This pulse creates a torque on the net magnetic moment vector which rotates it about the x-axis. This pulse can be tailored to rotate the moment 90° . When the pulse is turned off, the moment precesses around the static field in the z-direction. The angular frequency at which it precesses is a function of the applied field, and is known as the Larmor frequency. The Larmor frequency can be determined by the equation:

$$\omega = \gamma H \quad (2)$$

Where γ is the gyromagnetic ratio, which is a property of each isotope. This rotating moment creates a time-varying magnetic field in the x-y plane. In accordance with Maxwell's equations, the coil used to create the pulse which has its axis in the x-direction now has a voltage induced in it by the changing magnetic field. This signal is known as a free induction decay (FID).

B. Broadening

In the absence of energy exchange with the crystal lattice this precession would go on forever. As the net magnetic moment vector precesses, the microscopic magnetic moments see slightly different local magnetic fields and

therefore precess at slightly different rates. These differing precession rates cause the microscopic magnetic moments move ahead of or fall behind the average precessing vector. The vector sum of these individual moments decreases, causing the net magnetic moment to loose strength. The larger the variations in the magnetic field, the faster the moments will fan out and the more rapidly the FID will decay. This will result in a composite line of finite width. The time required for the spins to fan out is characterized by a scaling parameter called T_2 . This fanning out effect is shown in figure 1. The thick arrow represents the net moment and the thin arrows a sampling of the individual moments. The top drawing shows the moments shortly after the FID begins, while the bottom drawing represents a later time and shows the moments fanning out. This process is known as broadening. Two major interactions cause this broadening: 1) The dipole - dipole interaction, and 2) The nuclear electric quadrupole moment - electric field gradient (EFG) interaction. Although, these are not the only interactions that give width to the lines, they are the major sources of broadening in these experiments, hence the only ones to be considered in this report.

Broadening is quantised by calculating the second moment of the lineshape. The breadth of the line is

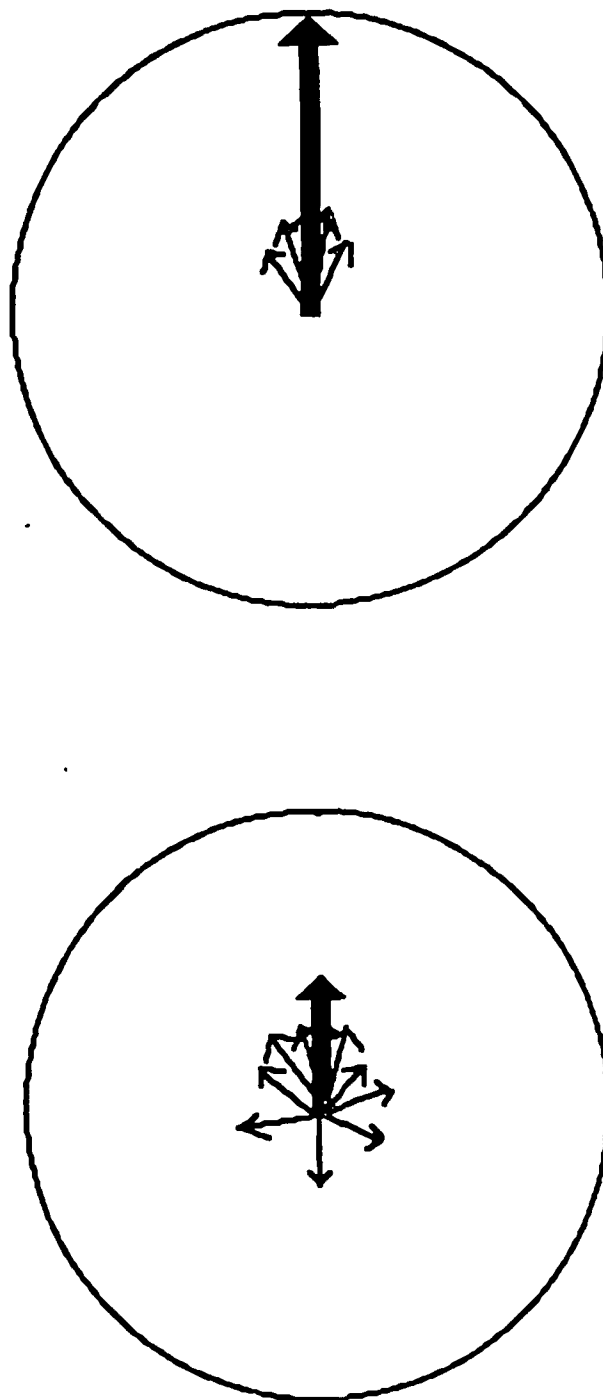


Figure 1. Net moment (thick arrow) and sampling of individual moments (thin arrows) shortly after pulse (above) and at a later time (below) showing fanning.

proportional to the second moment. A second moment is calculated by taking the sum of the intensity at every point on the lineshape multiplied by distance from that point to the center of the lineshape. We then normalize the moment by dividing by the total intensity in the lineshape. Second moments are calculated in units of energy squared, frequency squared, or magnetic field squared.

The dipole interaction is always present among magnetic nuclei. Each atom which has a non-zero spin has a magnetic dipole moment. These dipole moments act like small bar magnets. The magnetic field at any given nuclear site is the summation of the static magnetic field and the dipole fields of each of the other atoms in the crystal. Each individual moment is precessing at its Larmor frequency, further complicating the situation. Because the moments for any given isotope should all have the same Larmor frequency any given atom should be most strongly affected by the precession of the moments of the nuclei of the same isotope. This broadening by interaction with the same isotope is called like dipole broadening and is the most important part of the dipole broadening. The broadening from unlike moments (nuclei precessing at a different rate) is known as unlike dipolar broadening. Because the nuclei are not in phase, their effect on the magnetic field is

averaged over time and is not as strong. A further exchange effect which has the same form as the dipolar effects is called pseudodipolar broadening. The pseudodipolar effect in gallium arsenide has been shown to be negative, meaning that it cancels some of the dipolar broadening.³

The quadrupole interaction requires nuclei with a spin greater than $1/2$, and a non-zero EFG. Both isotopes of gallium, ^{69}Ga and ^{71}Ga , as well as the single isotope of arsenic, ^{75}As , have a spin $I=3/2$. Because gallium arsenide has a zinc blende structure, each gallium is surrounded by four arsenic atoms in a site of tetrahedral symmetry, and vice versa. At such a site the EFG is zero and there are no quadrupole effects.

Extended x-ray absorption fine structure (EXAFS) studies, by J. C. Mikkelsen, Jr. and J. B. Boyce have indicated that the indium atoms substitute into the gallium lattice while maintaining their characteristic In-As bond length, which is approximately 10% longer than the Ga-As bond length.⁴ This produces a strain in the crystal, destroying the tetrahedral symmetry and creating an EFG. The quadrupolar interaction thus created can be described by two parameters: 1) The quadrupolar coupling constant, Q_{cc} which describes the strength of the interaction, and the asymmetry parameter, η , which measures the deviation

from axial symmetry of the EFG. The frequency shifts caused by this interaction can be calculated by perturbation calculations carried to first or a higher order. A small, first order effect would create symmetrical satellites around the central peak. A stronger effect which produces second order changes would involve asymmetrical broadening of the central peak, as well as increasing the width of the first order wings and the separation of the satellites.

For atoms far from the impurity, the strain, and consequently the EFG, is small and changes very little from one shell of neighbors to the next. The satellites from these atoms cannot be resolved from each other or from the central peak. Instead, they blend together to form wings.

C. Echos

If a second pulse is applied so that the time (τ), between the leading edges of the pulses is greater than the pulse lengths, but less than the relaxation time of the system, an echo will be formed at a time (τ) after the second pulse. After the first pulse, the spins lose phase coherence in a time T_2 . The broadening mechanisms discussed above cause this dephasing. The echo forms because the second pulse rephases the spin system. The timing of

the echo depends on the pulse separation because the spins require as much time to return to their maximum coherence as they had to lose coherence. The spin-lattice relaxation time for the system is the amount of time required for the system to recover from the disturbing pulse and return to an equilibrium state. It is characterized by the parameter T_1 , which is a measurement of the time required for the system to give magnetic spin energy to the lattice as thermal energy, and is known as the spin - lattice constant. If the lengths of the two pulses are tailored properly, the echo contains the same information as the original FID. This is useful because the leading edge of the FID is buried in the pulse and the fastest decaying parts of the signal cannot be detected. These fast decaying parts of the FID which give the line most of its width. Because there is no pulse to mask it, the whole echo can be analyzed. The echo was frequency analyzed to produce a lineshape. The second moment of this lineshape could then be calculated. The top of figure 2 is an example of an echo and the bottom shows the same echo after the first part of it was deleted. It was this part of the echo that was transformed to produce the lineshapes.

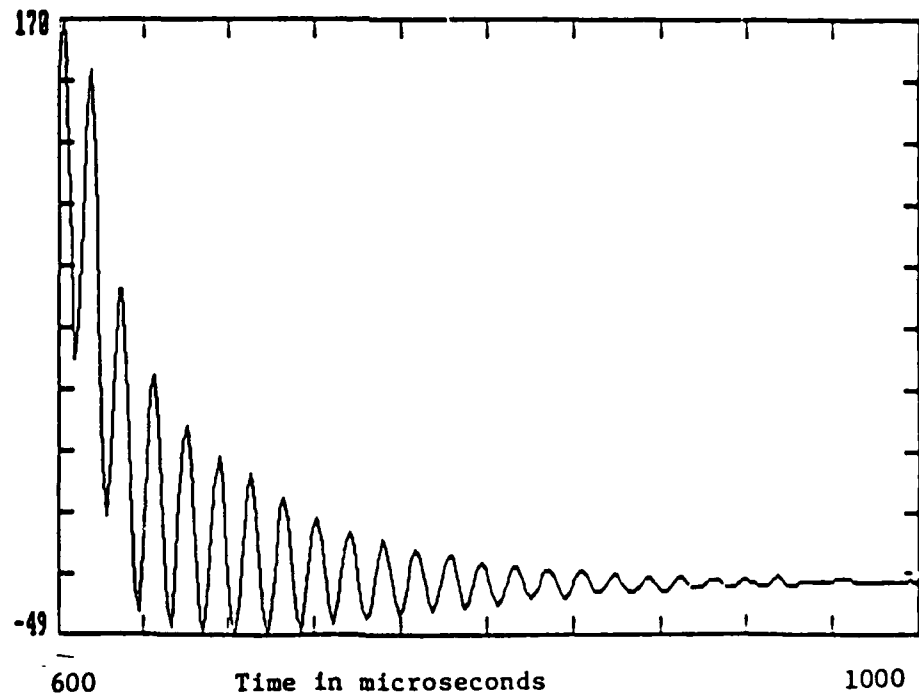
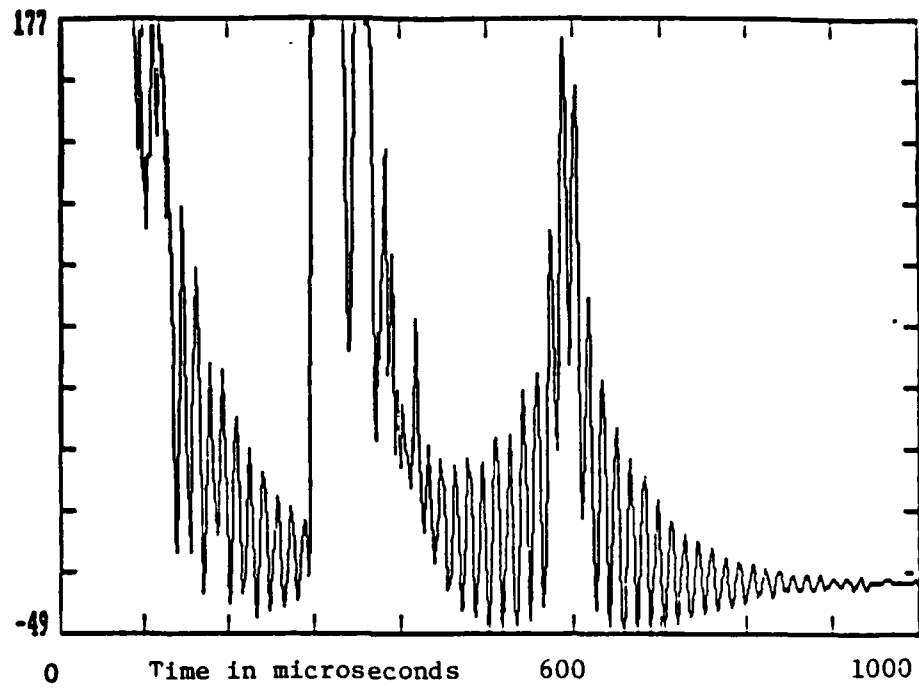
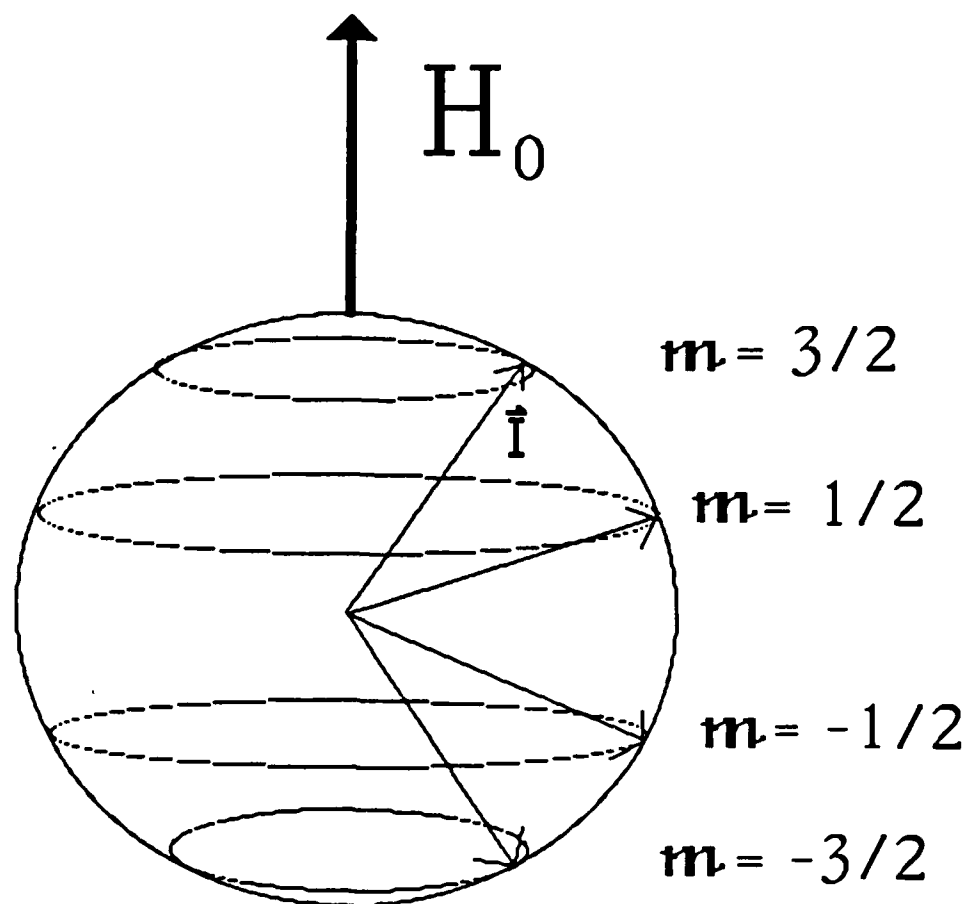


Figure 2. Echo (above) and that portion (below) of it that was transformed to determine lineshape.

III. Quantum NMR Theory

A. Zeeman Energies

The Hamiltonian is an expression for the total energy in a system. The Hamiltonian is linear, and thus a complex Hamiltonian can be broken down into its component parts. The simplest part of the Hamiltonian for GaAs NMR is the Zeeman energy, the energy associated with a nuclear spin in a static magnetic field. It is analogous to the splitting in the hydrogen spectrum when the light source is in a magnetic field. This splitting was first explained by the 19th century Austrian physicist whose name it bears. Both of the gallium isotopes and the single arsenic isotope are spin $3/2$. The z-component of this spin is quantized. The only accessible states are those where the z-component of spin is between $3/2$ and $-3/2$ in integral steps as shown in figure 3. The quantum number m , called the magnetic quantum number because it specifies the orientation of the magnetic moment of a nucleus with respect to a magnetic field is used to describe these states. If an external magnetic field (H_0) is applied, it defines the z-direction. The magnitude of the energy difference between any two states is independent of which values of m they are. The difference in energy is given by:



$$I = \sqrt{(3/2)(3/2 + 1)}$$

Figure 3. Spin states for a spin 3/2 nucleus in a magnetic field.

$$\Delta E = \gamma \hbar H_0. \quad (3)$$

The interaction between the magnetic field and the magnetic moments associated with the nuclear spin has the Hamiltonian⁵

$$\mathcal{H}_Z = -\vec{\mu} \cdot \vec{H}_0. \quad (4)$$

Where μ , the magnetic moment is

$$\vec{\mu} = \gamma \hbar \vec{I}. \quad (5)$$

Where γ is the gyromagnetic ratio, \hbar is Planck's constant divided by 2π , and \vec{I} is the spin vector of magnitude $\sqrt{I(I+1)}$. The Zeeman Hamiltonian gives a monochromatic resonance. To account for the width of a line, other interactions must be considered. The interactions which give width to a NMR line in III-V semi-conductors are the dipolar, the pseudodipolar, and the quadrupolar interaction. The effect of each of these will be examined in the following sections.

B. Dipolar Broadening

The dipolar interaction is an interaction between two nuclear dipole moments. The interaction energy between two nuclear magnetic dipoles with a separation \vec{r}_{12} is⁵

$$E = \frac{\vec{\mu}_1 \cdot \vec{\mu}_2}{r_{12}^3} - \frac{3(\vec{\mu}_1 \cdot \vec{r}_{12})(\vec{\mu}_2 \cdot \vec{r}_{12})}{r_{12}^5} \quad (6)$$

This energy can be summed over all the spins in the sample to get the Hamiltonian. The Hamiltonian for the dipolar interaction over a sample with n spins can be written as:⁵

$$\mathcal{H}_D = \sum_{i=1}^n \sum_{j=1}^n \left[\frac{\vec{\mu}_i \cdot \vec{\mu}_j}{r_{ij}^3} - \frac{3(\vec{\mu}_i \cdot \vec{r}_{ij})(\vec{\mu}_j \cdot \vec{r}_{ij})}{r_{ij}^5} \right] \quad (7)$$

Where $\vec{r}_{i,j}$ is the internuclear distance between atoms i and j , and $\vec{\mu}_i$ and $\vec{\mu}_j$ are the respective magnetic moments for these nuclei.

The dipolar contribution to the second moment of the lineshape is³

$$\langle H^2 \rangle = \sum r_{ij}^{-6} P_2^2(\theta_{ij}) = X + Y(\theta) \quad (8)$$

In the present experiment, the crystal is rotated about a $[110]$ axis and θ is the angle between the $[110]$ direction

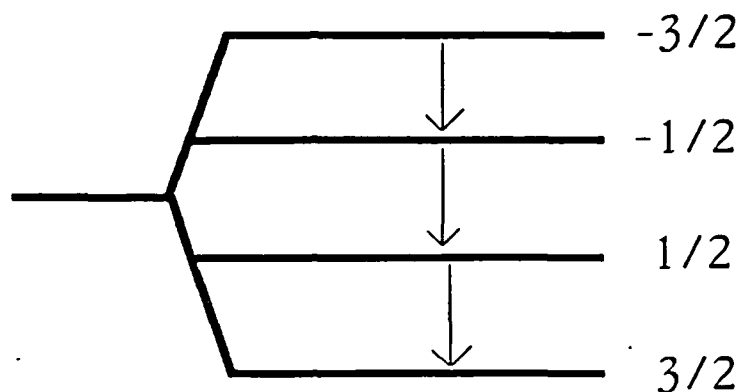
and the magnetic field. $P_2(\theta)$ is the second Legendre polynomial and contains both a constant term and a term which depends upon the angle between the magnetic field and the radius vector from the resonant nucleus to the nucleus producing the local magnetic field. Thus the dipolar interaction contains an isotropic part and a part which is dependent on the orientation of the crystal.

C. Quadrupolar Broadening

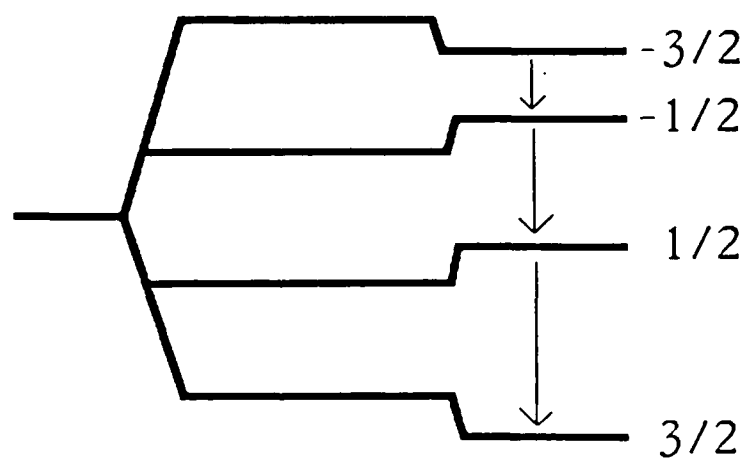
For nuclei of spin $1/2$ or more the quadrupole moment can interact with the EFG at the nucleus. This interaction alters the splitting between the levels so that it is no longer uniform, thus removing the degeneracy between the transitions. This is shown in figure 4. In this figure the amount by which the quadrupolar interaction alters the splitting is exaggerated for clarity. The energy difference between the two levels is now dependent on which two levels they are. The EFG is a 3×3 tensor whose components are the spatial derivatives of the components of the electric field (\vec{E}). This matrix can be diagonalized and the trace computed. The trace of the EFG tensor is given by

$$\text{Tr}(V_{ij}) = \frac{dE}{dx}x + \frac{dE}{dy}y + \frac{dE}{dz}z \quad (9)$$

No Quadrupolar Effect



$H = 0$ $H \neq 0$ \mathbf{H}



Quadrupolar Effect

Figure 4. Energy levels for a spin $3/2$ nucleus without (above) and with (below) first order quadrupole effects. Quadrupole effects exaggerated for clarity. Arrows indicate observable transitions.

Where dE_i/di is the partial derivative with respect to i of the component of the electric field in the i -direction. This trace is the divergence of the electric field at the resonant nucleus produced by everything except the resonant nucleus. Therefore, by Gauss' Law, the trace must equal zero. The EFG tensor can also be transformed to the principal axis system, where all off-diagonal components are zero. These constraints allow the Hamiltonian to be written in terms of two parameters.⁵

$$Q_{cc} = e^2 Qq/h \quad (10)$$

and

$$\eta = (dE_x/dx - dE_y/dy)/(dE_z/dz) \quad (11)$$

Where Q_{cc} is the quadrupolar coupling constant, η the asymmetry parameter, e is the magnitude of the charge on an electron, Q is the nuclear quadrupole moment, and $eq = dE_z/dz$. The quadrupole term of the Hamiltonian for an axially symmetric field can then be written as⁵

$$\mathcal{H}_Q = \frac{hQ_{cc}}{4I(2I+1)} \quad (12)$$

The Hamiltonian for the interactions we have already considered is

$$\mathcal{H} = \mathcal{H}_Z + \mathcal{H}_0 + \mathcal{H}_Q \quad (13)$$

If we consider the size of the various terms involved, we find that in this experiment the Zeeman splittings are on the order of 20 MHz, the quadrupolar splittings are of the order of 100 kHz for near neighbors, and the dipolar splittings are of the order of 1 kHz. Thus, the dipolar broadening can be approximated as a perturbation, and the Hamiltonian can be reduced to:

$$\mathcal{H} = \mathcal{H}_Z + \mathcal{H}_Q \quad (14)$$

When a Hamiltonian is composed of multiple terms and one term is much larger than the other, perturbation theory may be a useful method for obtaining a solution. If the larger term can easily be solved, or has already been solved, the smaller term can be considered as a perturbation to the results of the larger term. There are two possible cases here, (1) the Zeeman energy is much larger than the quadrupole energy, or (2) the quadrupole energy is much larger than the Zeeman energy. The second case is Nuclear Quadrupole Resonance, and is beyond the scope of this work. The first case applies here, so the quadrupole energy will be considered as a perturbation of the Zeeman energy.

The solution to the Zeeman Hamiltonian gives a

resonance at the frequency

$$\nu_0 = \Delta E/h \quad (15)$$

Where ΔE is the difference in energy between two adjacent states. This frequency, ν_0 , is the Larmor frequency.

If a radio-frequency (rf) pulse of magnitude H_1 is now applied perpendicular to the static field (H_0), transitions are induced. If the rf field is in the x-direction, the Hamiltonian for the duration of the pulse can be written as⁵

$$\mathcal{H}_{\text{rf}} = -\gamma \hbar I_x H_1 \cos(\omega t) \quad (16)$$

where ω is the angular frequency of the rf field. The pulse is finite in time, and thus consists of a finite bandwidth of frequencies, the bandwidth of which is proportional to the inverse of the length of the pulse. This allows the pulse to cause transitions over a range of frequencies. The probability of a transition between states m and m' is proportional to⁶

$$1/4 \left| \sqrt{I(I+1)-m(m+1)} \delta_{m',m+1} + \sqrt{I(I+1)-m(m-1)} \delta_{m',m-1} \right| \quad (17)$$

Because the delta function is zero except when m'

equals $m+1$ or m' equals $m-1$, the only allowable transitions are those between adjacent levels. The probability that a given moment will have an upward transition from the m^{th} to the $(m+1)^{\text{th}}$ level by absorbing a photon is exactly the same as that for a moment in the $(m+1)^{\text{th}}$ level to decay to the m^{th} level by stimulated emission of a photon. Before the pulse is applied, the system is in thermal equilibrium. The numbers of nuclei in each of the spin states, therefore, obeys a Boltzmann distribution, where the number of nuclei in each state decreases exponentially as the energy of the state increases. Because there are more nuclei in the lower states, the net result is an increase in the number of nuclei in the upper levels. As more moments move up to higher energy levels, the populations even out. When the pulse is removed the moments will try to decay back to their equilibrium levels. As they do so they will emit radiation at a frequency

$$\nu_0 = \Delta E/h. \quad (18)$$

The correction for the quadrupolar interaction to second order as calculated by Wolfe, Kleine, and Story is⁷

$$\nu = \nu_0 + \nu_Q A(m-1/2)/2 + \nu_Q \beta C/72 \quad (19)$$

Where

$$\nu_Q = \frac{3Q}{2I(2I-1)} \quad (20)$$

β is defined as ω_Q/ω_0 , and A and C are complicated functions of m, I, θ , ϕ , and η . θ and ϕ are the Euler angles of the magnetic field with respect to the principal axis system of the EFG tensor. The m indicates the upper level of a transition from the m to m-1 nuclear level. If the strength of the quadrupolar interaction is low enough the last term may be neglected, resulting in first order broadening. Because (m-1/2) is zero for the m= 1/2 to -1/2 transition, the central transition in Ga and As is unaffected. Also, for the m=3/2 to 1/2 and m=-1/2 to -3/2 the first terms are the additive inverses of each other resulting in symmetrical wings or satellites, depending on the environment of the radiating nuclei. For stronger interactions second order terms are necessary. The second order term effects the central transition as well as the satellite transitions, creating an asymmetrical line.

D. Pseudodipolar Broadening

The pseudodipolar interaction involves electron coupling of the nuclear spins of neighboring atoms. It is

called pseudodipolar because its effects have the same functional form as the dipolar effects. The pseudodipolar contribution to the second moment summed over the entire crystal is given by³

$$\langle E^2 \rangle = 2h^2 \Gamma_s \sum \tilde{B}_{ij} (2 + \tilde{B}_{ij}) r_{ij}^{-6} P_2^2(\theta_{ij}) \quad (21)$$

Where \tilde{B}_{ij} is the pseudodipolar coupling constant, and Γ_s is the gyromagnetic ratio for the non-resonant nuclei. Because the pseudodipolar interaction is electron coupled, it has a very short range⁸, and it can be assumed that only the nearest neighbors couple effectively. The coefficients \tilde{B}_{ij} are independent of θ_{ij} and may be pulled out of the summation and replaced by the nearest neighbor coupling constant, \tilde{B}_{nn} . The pseudodipolar contribution to the second moment may then be rewritten as³

$$\langle E^2 \rangle = 2h^2 \Gamma_s^2 \tilde{B}_{nn} (2 + \tilde{B}_{nn}) (4/a_o \sqrt{3})^6 f(\theta) \quad (22)$$

With the approximation that only the nearest neighbor shell affects the pseudodipolar interaction, it has the same angular dependence as the angular dependent term of the dipolar interaction, but there is no isotropic term.

IV. Experiment

The experiment was performed on two single crystal n-type semiconductors. Both samples were donated by Westinghouse to the Naval Research Laboratories in Washington D.C.. One had an indium concentration of $1\text{--}2 \times 10^{18} \text{ cm}^{-3}$, and a resistivity of $4 \times 10^7 \text{ } \Omega\text{-cm}$; the other, a more heavily doped sample, had an indium concentration of $7 \times 10^{19} \text{ cm}^{-3}$, and a resistivity of $4.4 \times 10^7 \text{ } \Omega\text{-cm}$. The sample was prepared so that the $[110]$ axis of the sample could be orientated perpendicular to the magnetic field, and the sample was rotated about this axis.

Measurements were made with a standard pulsed NMR system. The magnetic field was provided by a Varian Associates electromagnet with a Fielddial Mark II regulator/power supply. The gated pulse generator was a Matec model 5100 with a model 515A gated power amplifier. The preamp was a Matec model 235, and the receiver/detector a Matec model 625. Several coils for the probe were wound of #18 lacquer covered copper wire.

Because the sample is piezoelectric, a transient signal was observed following each pulse. Also, the time constant of the system was such that the system took seventy-five to eighty microseconds to recover from the rf pulse, obscuring the rapidly decaying part of the FID. To

avoid this loss of information, all measurements were made on the echos following a 90- τ -60 pulse sequence. The numbers refer to the pulse length, which is described by the number of degrees the net magnetic moment vector is rotated. This sequence was selected so that the central transition and satellites were emphasized in the same proportions as in the FID.¹

The magnet and table acted as an antenna picking up an unwanted signal of several times the magnitude of the NMR signal. Much of this noise was being generated by the IBM personal computer used to analyze data, thus the all data were taken with the computer off. Several grounding methods were tried to reduce the remaining noise. The most effective consisted of a screen box for the probe which was grounded to the pole faces of the magnet. Strong signals of unknown origin were detected at various frequencies, the strongest at 12.6 MHz. To avoid these signals the data was taken in the neighborhood of 18MHz. This required rewinding the coil in order for it to be tuned at the proper frequency.

The signal-to-noise ratio (S/N) of the echo was approximately 3. Signal averaging, done with a Gould digital oscilloscope which averaged 256 traces, was used to improve this to about 50. Each trace consisted of 1024 data points converted to a digital signal with an eight-bit

analog-to-digital converter. The echoes were then fourier analyzed to determine a lineshape. The second moment was calculated directly from this lineshape. Programs were written in basic to transfer data from the oscilloscope to the computer and to calculate the second moment of the lineshape.

V. Results

Rotational patterns for ^{69}Ga were taken for two different samples. The second moments were taken directly from the lineshape. Only those parts of the lineshape more than 10% of the peak height above the baseline were used in calculating the moments. This creates a slight narrowing in the results, but poor (S/N) precluded accurate measurements near the base. An example of an echo signal and its corresponding lineshape for both of the samples studied are shown on the following pages, in figures 5 and 6. First order quadrupolar broadening is easily visible as wings in the more heavily doped sample, and the beginnings of small wings are visible in the lightly doped sample.

Hester, Sher, Soest, and Weisz have shown that, assuming first order broadening, the angular dependance of the second moment can be fit to the function³:

$$\langle H^2 \rangle(\theta) = C + Df(\theta). \quad (23)$$

Where

$$f(\theta) = 2\cos^2(\theta) - 1.5\cos^4(\theta) \quad (24)$$

The isotropic part, C, is from the dipolar and exchange mechanisms, while the contributions to the constant D are from the dipolar, pseudodipolar, and quadrupolar mecha-

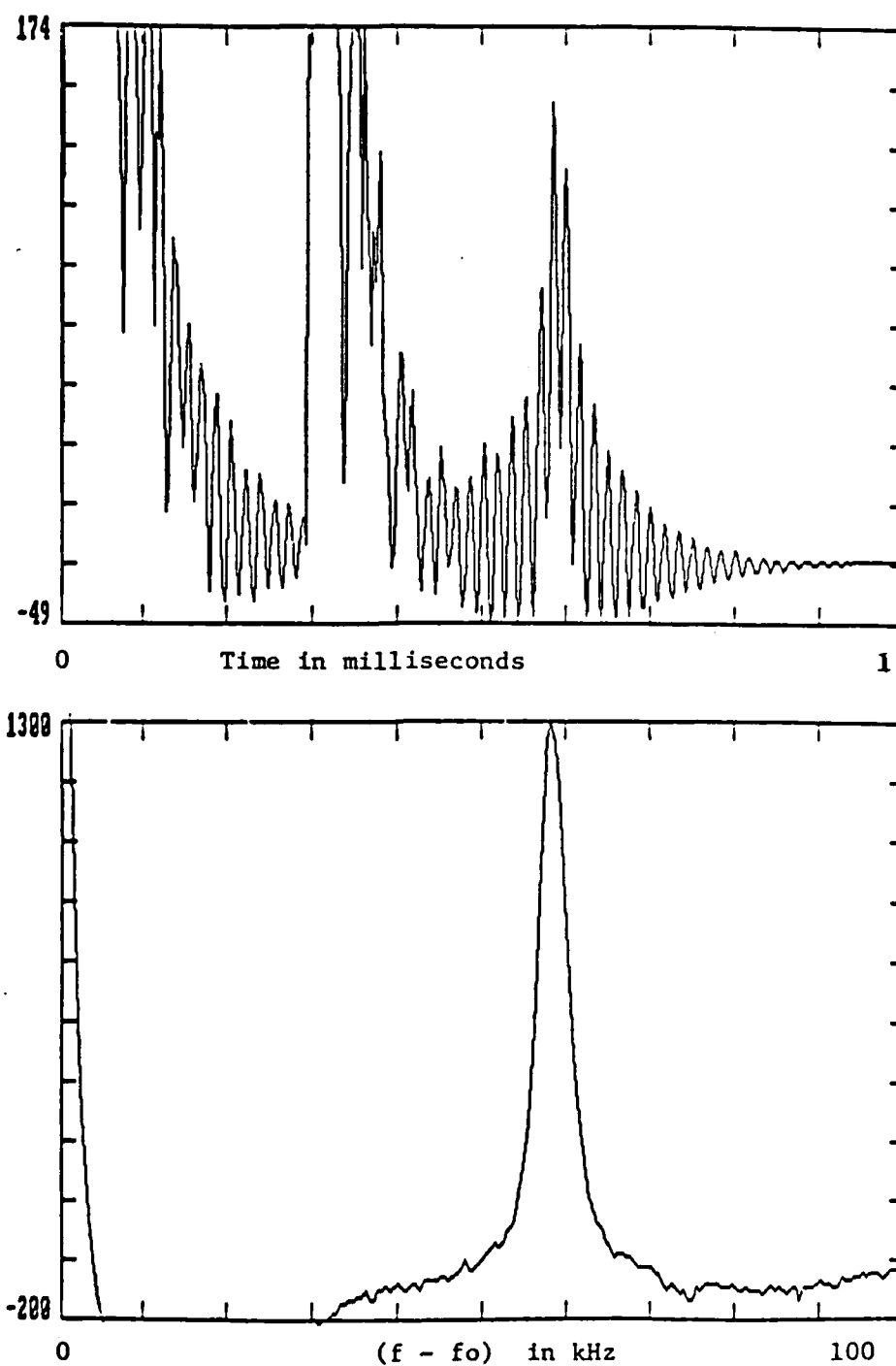


Figure 5. Echo (above) and lineshape (below) of ^{67}Ga for sample with $1-2 \times 10^{16} \text{ In/cm}^2$.

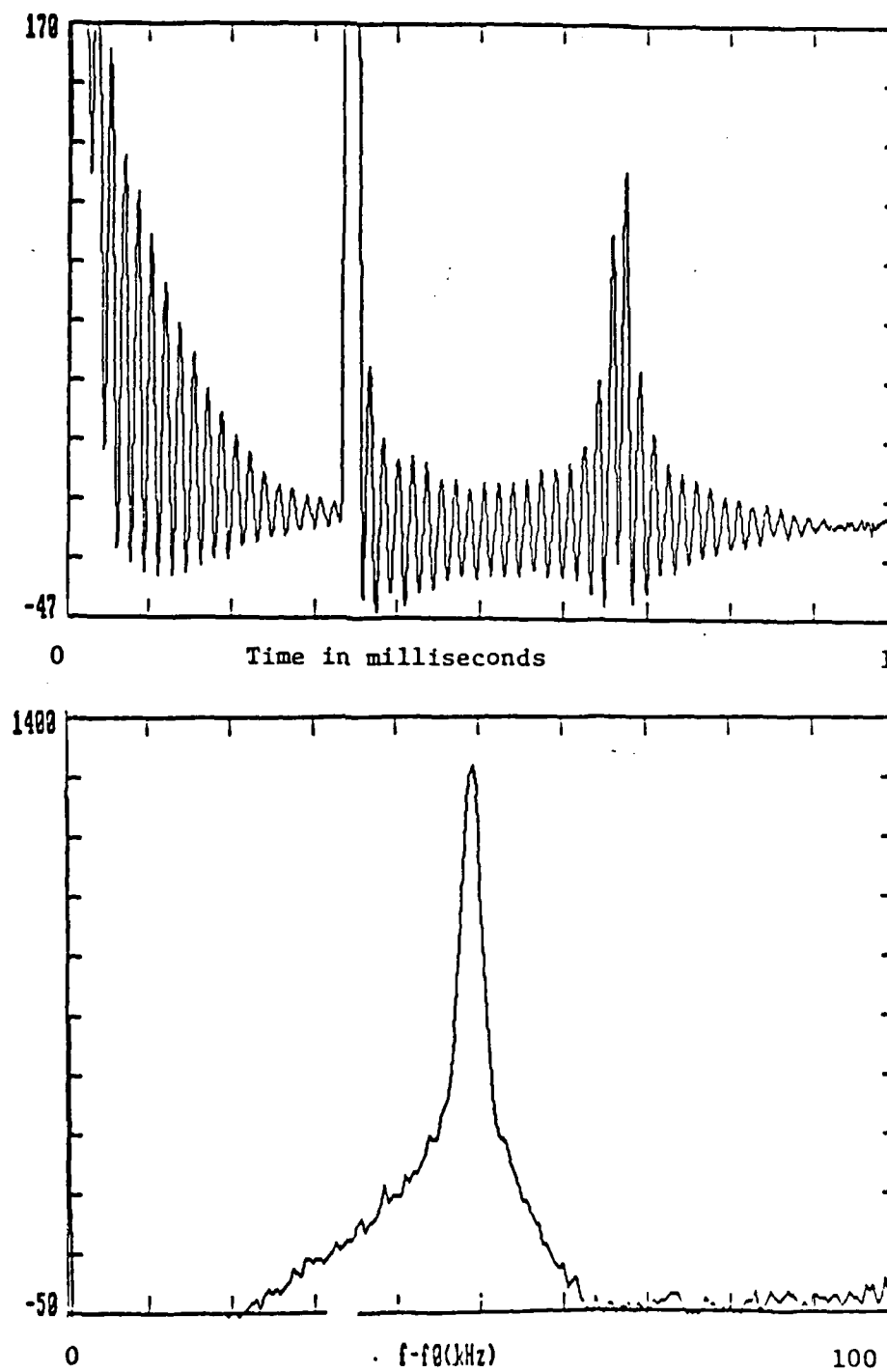


Figure 6. Echo (above) and lineshape (below) of ^{67}Ga for sample with $7 \times 10^{18} \text{ In/cm}^3$.

nisms.³ Data were taken at ten orientations spanning 90° . The second moments of both samples plotted vs the angle between the magnetic field and the [110] direction is shown as figure 7. The smooth curves represent a fitting to the function above using the fitting parameters C and D shown in table 1, below. The fitting was an interactive graphics fit where the uncertainty describes the variations in the parameters necessary to make a noticeable change.

TABLE 1

sample	In/cm ³	C	D
G0353-1174	$1-2 \times 10^{18}$	$2.7 \pm .1$	$2 \pm .2$
G0301-1198	70×10^{18}	$8 \pm .5$	14 ± 2

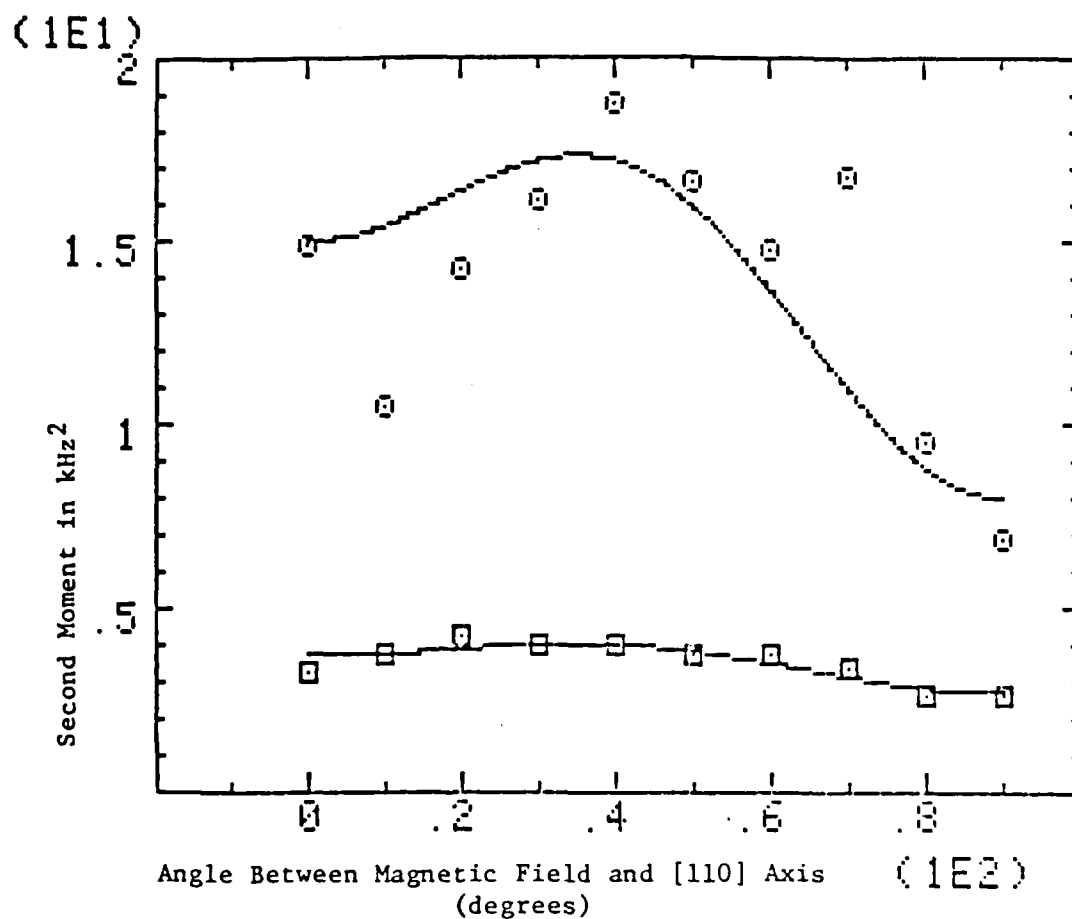


Figure 7. Rotational pattern for second moments of ^{69}Ga .
 Smooth curves represent fitting to function
 $C + D(2\cos\theta^2 - 1.5\cos\theta)$ using parameters from Table 1.
 Upper curve is for sample with $7 \times 10^{18} \text{ In/cm}^3$
 Lower curve is for sample with $1-2 \times 10^{18} \text{ In/cm}^3$

VI. Discussion of Results

The results of this study support first order quadrupolar broadening in the two samples investigated. No second order broadening effects were observed in this study. The second moments found agreed qualitatively with those found by Hester, Sher, Soest, and Weisz in their angular dependance.³ However, the moments found in this study were much larger, especially the isotropic terms.

The larger moments observed in this study came from three causes. First the sample used by Hester et al. was silicon doped. The non-isovalent nature of the silicon causes charge centers within the crystal. The electric field gradient then is dominated by the electric field caused by the charged impurities, with the contribution from crystalline strain being negligible. The EFG of a point charge follows an inverse cube law. A charged impurity also has an induced EFG caused by the relative displacement of the sublattices and the distortion of the valence orbitals. The induced EFG is proportional to the electric field at the site, and has an inverse square dependence. The net effect is that the inverse square induced EFG dominates the inverse cube EFG of the charged impurity. Because the indium dopant is isovalent the EFG in this study was instead caused by the strain in the

crystalline lattice, .

The elastic continuum approximation does quite well in simulating first order quadrupolar broadening in isovalently doped III-V semiconductors.⁹ An elastic continuum model predicts that the strain induced EFG falls off as the cube of the distance from an impurity. Also, the dopant level was several orders of magnitude lower in the silicon doped sample than in the indium doped samples used in this study. Even though the level of doping was much lower for the silicon doped sample, the less rapid diminishing of the silicon's EFG should at least partially make up for it's fewer numbers, because charged impurities are thirty times as effective in causing quadrupolar broadening as isovalent impurities.

The third reason for the larger moments reported here compared to Hester et al. is that this study used spin echos to calculate the moments instead of free induction decays. Preliminary investigations of FIDs taken in this laboratory also gave lower moments. Moments calculated for both samples from FIDs taken in this study had second moments of about two kHz². The pulse and associated ring down masked the first fifty to eighty micro seconds of the FID. This very first part of the FID contains the rapidly decaying parts of the signal which give the line much of its width. The echo was composed of two identifiable

parts: 1) A fast decaying part which gave a spike near the temporal center of the echo and 2) a more slowly decaying part which gives the narrow part of the absorption line when transformed.

One feature of the signals that could not be satisfactorily explained was in the echo of the lightly doped sample. The echo rose up above the baseline, and appeared to have some sort of exponential decay term added into the signal. A similar behavior was obtained in the FID. Proposed explanations for that signal include that it was 1) a ring down of the pulse, or 2) a piezoelectric response.³ The pulse had been off for several hundred microseconds when the echo occurs, eliminating the ring down as a cause. Also with no external electric field being applied at the time the echo was being observed, the piezoelectric effect cannot cause for the observed behavior. The possibility exists that it could be a magnetostrictive effect, but more experiments would have to be done before this could be definitely stated.

The experimentally determined second moments of the gallium arsenide lineshapes found in this study show first order quadrupolar broadening that supports an elastic continuum model of the strain in GaAs:In. The dependance of the moment on the orientation of the crystal in the magnetic field is qualitatively the same as that determined

by Hester et.al.. However, the moments found in this study are much larger, especially the isotropic terms. The major reason for the larger moments in this study is that the lineshapes calculated in this study were determined from spin echoes instead of from free induction decays.

NOTES

1. D. J. Treacy (private communication), (1987).
2. F. Bloch, Phys. Rev. 70, 460(1946).
3. R. K. Hester, A. Sher, J. F. Soest and G. Weisz, Phys. Rev. B 10, 4262(1974).
4. J. C. Mikkelsen, Jr. and J. B. Boyce, Phys. Rev. B 28, 7130(1983).
5. G. E. Jellison, Ph.D. Thesis, Brown University(1971).
6. C. P. Slichter, Principles of Magnetic Resonance, (Harper and Row, New York, 1963).
7. F. Wolfe, D Klein and H. S. Story, J. Chem. Phys 53, 3538(1970).
8. N. Blombergen and T. J. Rowland, Phys. rev. 97, 1679(1955).
9. W. E. Carlos, S. G. Bishop and D. J. Treacy, Appl. Phys. Lett., 49, 528(1986).

END

8-87

DTIC